



## Original Article

## Fabrication and Characterization of COL/PVA Nanofiber Scaffolds for Soft Tissue Engineering

Yalda Jahanbani<sup>1,2</sup>, Soodabeh Davaran<sup>1,\*</sup> , Mehdi Yousefi<sup>3</sup>, Leila Roshangar<sup>4</sup>, Parvin Bastani<sup>5</sup>, Jamileh Kadkhoda<sup>1</sup>

<sup>1</sup>Department of Medicinal Chemistry, Faculty of Pharmacy, Tabriz University of Medical Sciences, Tabriz, Iran

<sup>2</sup>Student Research Committee, Tabriz University of Medical Sciences, Tabriz, Iran

<sup>3</sup>Department of Immunology, School of Medicine, Tabriz University of Medical Sciences, Tabriz, Iran

<sup>4</sup> Tabriz University of Medical Sciences, Tabriz, Iran

<sup>5</sup>Obstetrics and Gynecology Department, Al-Zahra Hospital, Faculty of Medicine, Tabriz University of Medical Sciences, Tabriz, Iran

### ARTICLE INFO

#### Article history

Submitted: 2023-05-05

Revised: 2024-04-22

Accepted: 2024-05-25

ID: CHEMM-2405-1794

Checked for Plagiarism: Yes

Language check: Yes

DOI: 10.48309/CHEMM.2024.455838.1794

### KEYWORDS

Soft tissue engineering

Electrospinning

Nanofiber scaffolds

### ABSTRACT

Development of new biomaterial-based approaches for regeneration of soft tissues and organs such as heart, brain, uterine, ovarian, and others has received much attention in recent years. Here, we explain the stages of design and development of the biocompatible Collagen/Polyvinyl alcohol (COL/PVA) nanofiber scaffolds to transfer human umbilical cord mesenchymal stem cells (HUC-MSCs) to damaged soft tissue. In this study, by optimizing the percentage ratio of COL to PVA, the need for a cross-linking process to maintain the nanofibers' stability in aqueous environments was eliminated and this strategy significantly increased the biocompatibility of the synthesized nanofibers. The chemical structure of synthesized scaffolds was evaluated by Fourier-transform infrared spectroscopy (FT-IR). In addition, other physicochemical and biological aspects of the fabricated scaffolds, including nanofiber diameter, *in vitro* degradation, swelling behavior, mechanical properties, morphologies, and biocompatibility were surveyed. Physicochemical assessments showed that un cross linked 60/40 COL/PVA nanofiber scaffolds had a successful performance in terms of morphology and stability. Furthermore, these scaffolds had no toxicity on HUC-MSCs. Therefore, study was continued with the most ideal percentage composition of the prepared nanofiber scaffolds. Scanning electron microscope (SEM) images showed proper cell adhesion and distribution of HUC-MSCs throughout the nanofiber scaffolds.

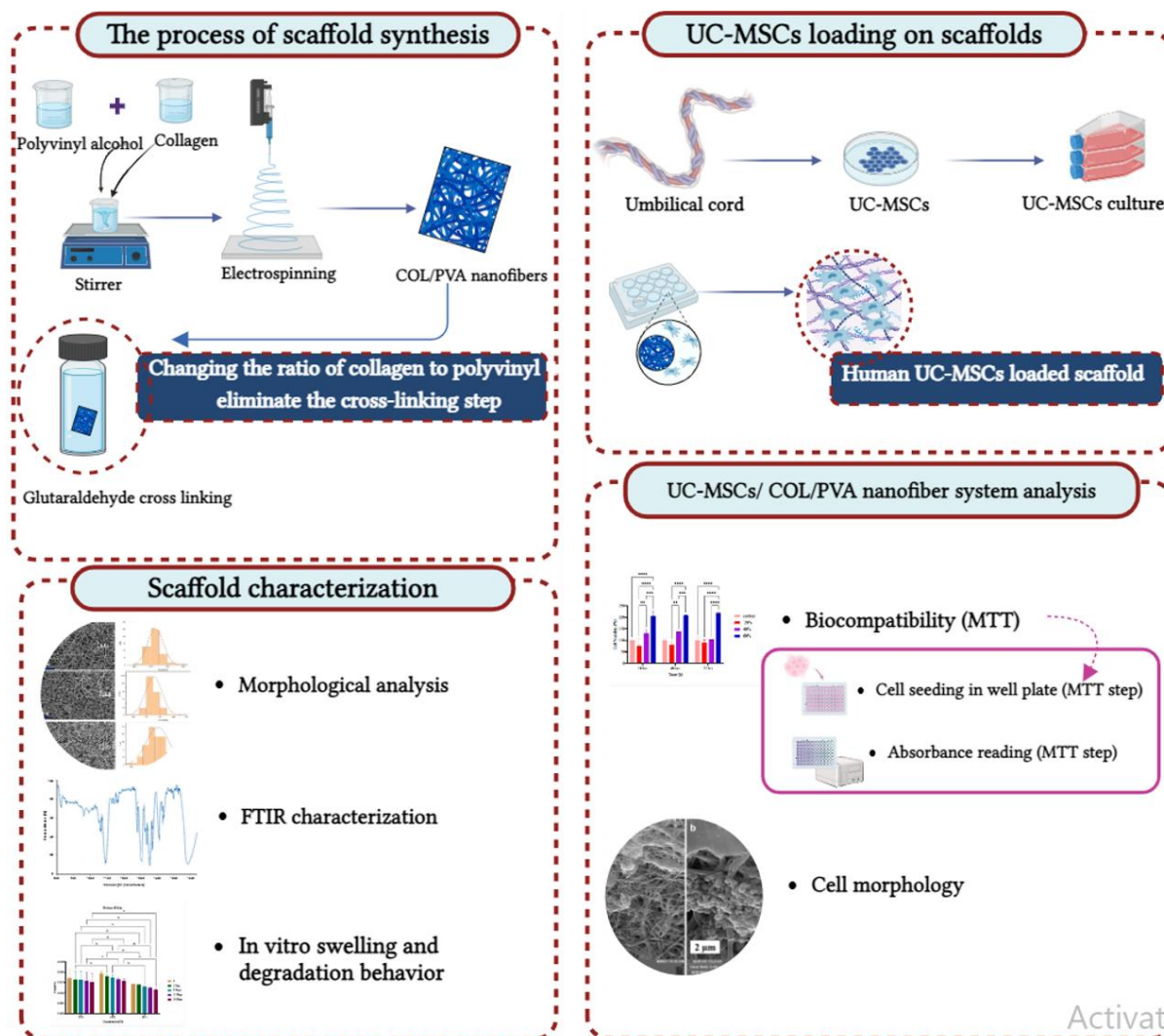
\* Corresponding author: Soodabeh Davaran

E-mail: [s.davaran2018@gmail.com](mailto:s.davaran2018@gmail.com)

© 2024 by Sami Publishing Company

This is an open access article under the [CC BY](https://creativecommons.org/licenses/by/4.0/) license

GRAPHICAL ABSTRACT



**Introduction**

Soft tissue engineering focuses on the repairing and regeneration of soft tissues and organs of the body and is developing rapidly. Tissue engineering emerged in the 1980s, as researchers sought to develop methods to regenerate functional tissues. Initially, the focus was on hard tissues such as bone, but attention gradually shifted to soft tissues. In recent years, studies in the field of soft tissues and organs regeneration and repairing such as endometrium [1], uterus [2], ovary [3], skin [4], kidney [5], and nerve [6] using tissue engineering technology have received much attention. Specifically, technologies based on biomaterials in the field of reproductive system tissue engineering have provided very promising preliminary results

[7,8]. Adult stem cells derived from various sources such as umbilical cord (UC), bone marrow (BM), and menstrual blood (Men) showed very high potential for the regeneration of different tissues [7,9,10]. However, the direct transfer of mesenchymal stem cells (MSCs) to desired position faces various challenges that peruse researchers to overcome these complications. High rate of cell death through necrosis and apoptosis immediately after transplantation is one of the most important problems [11]. To solve this challenge and improve the retention and survival of transferred cells, MSCs can be encapsulated in biomaterials such as hydrogels and scaffolds [12]. These biomaterials by simulating natural extracellular matrix (ECM) create an ideal environment for the survival and attachment of cells [13,14]. Tissue

engineering seeks to rebuild partial and complete tissues through these biomaterials and stem cells [15]. Studies have shown that natural and synthetic polymers combination can be a suitable option for making scaffolds with the expected characteristics [16-18]. Of course, achieving a structure with appropriate morphology, strength, and flexibility is one of the challenging issues regarding soft tissue engineering scaffolds. Collagen/ Polyvinyl alcohol (COL/PVA) nanofiber scaffolds prepared by electrospinning method as natural and synthetic polymers combined scaffolds have been highly regarded in this field due to their similarity to the ECM of native body tissues [19]. COL as a natural polymer and one of the important components of native ECM tissue is widely used in scaffold construction. Existence of Arg-Gly-Asp (RGD) peptide sequences as cell adhesion sites and matrix metalloproteinase (MMP) as biodegradation sites have given a unique bioactivity to this substance [13]. Compared with its excellent biological properties, COL faces challenges regarding mechanical properties and structural stability. Using physical and chemical cross-linking processes and combining collagen with a stronger synthetic polymer seems to be a suitable solution to these shortcomings [20,21]. Presence of PVA as a FDA approved synthetic polymer with collagen in the scaffold structure can provide improved mechanical stability and controlled degradation properties [22]. In addition, COL/PVA scaffolds are usually cross-linked by glutaraldehyde (GA) to improve water solubility [23]. Despite the widespread use of glutaraldehyde as a traditional cross-linking agent of scaffolds, many studies show that GA components on the surface of GA cross-linked scaffolds causes the induction of cell apoptosis and as a result reduces the biocompatibility of the synthesized scaffolds [21,24]. In general, most currently used cross-linker agents have limited potential to cause toxic effects [25]. It seems that eliminating the use of cross-linker agents in the synthesis of scaffolds can have a significant effect on improving the biocompatibility of these scaffolds.

In this study, we assumed that natural and synthetic polymers combination lead to

synthesize of scaffolds with satisfactory physicochemical features and scaffold-cell interactions. Furthermore, by optimizing the ratio of these polymers, the cross-linking stage can be eliminated. As mentioned previously, use of stem cells loaded scaffolds is a new and promising approach for healing damaged organs and tissues [7,26-27].

## Experimental

### Materials

Polyvinyl alcohol; PVA (88%, MW = 88.000–98.000 D), glutaraldehyde (25% aqueous solution), MTT (3-(4, 5-dimethylthiazol-2-yl) - 2, 5- diphenyl tetrazolium bromide), and phosphate buffer solution (PBS) were purchased from Sigma- Aldrich (USA). Fetal bovine serum (FBS), Dulbecco's modified Eagle's medium (DMEM), penicillin and streptomycin, and trypsin- EDTA were purchased from Life Technologies (GIBCO). Rat tail type I collagen was purchased from Fannavar Nano-Meyar Shaya company. Analytical grade of solvents and reagents were purchased from Merck Inc. (Germany).

### Preparation of Electrospinning Solutions

To prepare the COL/PVA electrospinning solutions, the PVA and COL solutions were prepared separately and so on mixed together. The PVA 10 wt. % solution was achieved by dissolving 2 grams of PVA powder in deionized water at 80 °C for 1.5 h under stirring condition, and then 0.2 grams of COL powder was dissolved in 10 mL of demineralized water containing 0.5 M acetic acid to prepare the COL solution. In the next step, COL solution was mixed with PVA solution at the COL/PVA volume ratios (V/V) of 20/80, 40/60, 60/40, and stirred for 2 hours at ambient temperature to obtain homogeneous electrospinning solutions.

### Electrospinning Process

To implement electrospinning process, pre-prepared solutions were placed into a 5 mL plastic syringe equipped with a blunt-tipped 21-

gauge stainless steel needle. The applied voltage and injection rate were adjusted at 27 kV and 0.3 mL/h, respectively. Horizontal distance of needle tip and aluminum foil collector for nanofibers collection were adjusted to 8 cm and the rotating speed was set on 360 rpm. Conditions of electrospinning process was set at  $25 \pm 2$  °C and  $30 \pm 1\%$  relative humidity [28,29]. Electrospun nanofiber scaffolds to remove the residual solvent were subjected to vacuum conditions for 24 hours at room temperature. It is necessary to mention, electrospinning ability of prepared solutions was strongly influenced by the ratio of COL to PVA. By increasing COL ratio, the electrospinning ability of prepared solutions was drastically decreased, while the presence of COL in scaffold improves many of its biological properties. It seems very important to achieve the optimal concentration of COL in the scaffold structure.

#### *Cross-Linking of Electrospun COL/PVA Nanofibers*

Both COL and PVA are hydrophilic polymers, and hence COL/PVA nanofibers structure is rapidly destroyed in water environments [30]. To protect nanofibers from dissolving in aquatic environments, nanofiber mats should be cross-linked. To prepare cross-linking solution 2 % glutaraldehyde, 1 % ethanol, and 0.1 % hydrochloric acid was added in 100 grams of acetone. The glutaraldehyde cross-linking process was carried out by placing the prepared nanofibers with their aluminum foils in a sealed jar containing cross-linking solution for 30 min. Afterwards, for blocking the residual glutaraldehyde aldehyde groups, nanofiber scaffolds were immersed in glycine aqueous solution (1%, v/v), and incubated for 2 hours at 37 °C, and then the fibers were rinsed with deionized water and placed in the vacuum oven for 24 hours at room temperature.

#### *Characterization of Nanofibrous Scaffolds*

##### *Fourier-Transform Infrared Spectroscopy (FTIR) Characterization*

The chemical structure of COL/PVA nanofibers has been examined using FT-IR. Range of 4000–450  $\text{cm}^{-1}$  was used on the ATR-FTIR (BRUKER, Tensor 27).

##### *Field Emission Scanning Electron Microscopy (FESEM) Analysis of COL/PVA Nanofibers*

After the gold coating stage, the morphologies of un-cross linked and cross-linked COL/PVA nanofibers were characterized by FESEM (FESEM; Sigma VP, ZEISS, Germany). About all synthesized nanofibers the average nanofiber diameters were deliberated by ImageJ software.

##### *Mechanical Analysis*

The mechanical tests of un-cross-linked and cross-linked COL/PVA nanofibers were investigated by a Zwick tensile testing machine (Z010, Zwick/Roell, and Ulm, Germany). For this test, the prepared nanofibers were cut with dimensions (10 mm × 10 mm), and 10 N compression was applied with loading rate of 5 mm/min. The analysis was performed at ambient temperature. Stress-strain diagrams were drawn for each of prepared samples, and Young's modulus was deliberated.

##### *In Vitro Swelling and Biodegradation Behavior of the COL/PVA Nanofibers*

The swellability of the prepared nanofibers was evaluated by swelling experiments. The prepared samples were initially cut with dimensions ( $1 \times 1 \times 1 \text{ cm}^3$ ) and their weights were measured. Thereafter nanofibers at 37 °C were immersed in a phosphate buffer solution (PBS, pH = 7.4). The scaffolds were taken out from the PBS solution after a certain period of time and their wet weights  $W_w$  were measured. It is worth mentioning that before  $W_w$  measuring removing excess water of samples by filter paper is necessary. Swelling percent ( $\%S_w$ ) was calculated using Equation (1) [31].

$$\left(\frac{W_w - W_d}{W_d}\right) \times 100 \quad (1)$$

To investigate the biodegradability of synthesized scaffolds, the scaffolds were cut in dimensions ( $1 \times 1 \times 1 \text{ cm}^3$ ) and weighed, and then placed in PBS solution for a certain period. After the specified time, the scaffolds were removed from the PBS solution, dried, and weighed, the values are the mean  $\pm$  standard deviation ( $n = 3$ ). Weight loss percentage was measured using Equation (2) [32].

$$((W_w - W_t) / W_d) \times 100 \quad (2)$$

### Cell Culture Studies

Before starting the cell culture step, it is necessary to sterilize all the synthesized scaffolds [33]. For scaffolds sterilization, the prepared samples were placed in 12-well cell culture plates and immersed for 30 min in a 70% ethanol solution [34]. To completely remove ethanol from nanofibers, after ethanol evaporation, synthesized nanofibers were washed three times with PBS solution. After going through these steps, to perform the last stage of sterilization UV-lamp was used, and then samples were incubated over night at 37 °C in Dulbecco's modified Eagle medium (DMEM) [34].  $2 \times 10^6$  HUC-MSCs was dripped onto each scaffold. Cell culture medium was also refreshed every three days.

### Cell Morphology Studies

After 3 days of cell culture, morphology of cultured cells on scaffolds was analyzed by SEM. For SEM imaging, the steps were taken in this order: The cell-seeded nanofiber scaffolds after PBS washing were fixed in 2.5% glutaraldehyde solution. In the next step, sequence of ethanol/water solutions with volume ratios of 50, 70, 90, and 100% to dehydration of scaffolds were used and so on prepared samples were dried at 37 °C.

### In Vitro Biocompatibility Evaluation

Biocompatibility of synthesized nanofibers was investigated by MTT assay. To this aim, HUC-MSCs were seeded on sterilized scaffolds with a

density of  $2 \times 10^6$  cells per scaffold in 96-well plates. HUC-MSCs in scaffold-free media were considered as control group. All tests were repeated 3 times for all samples. After 24, 48, and 72 hours of incubation, the media was refreshed by 150  $\mu\text{L}$  of complete cultivation environment, and 50  $\mu\text{L}$  of MTT (3 mg/mL in PBS) solution was added and incubated for 3 hours. After supernatant removing, 200  $\mu\text{L}$  of DMSO was added to each well. Afterwards, for dissolving the formed formazan crystals, plates were shaken for 45 min and 100  $\mu\text{L}$  of supernatant was moved to another 96-well plate. Eventually, absorbance was measured at 570 nm by plate reader.

### Statistical Analysis

All results were reported as the mean  $\pm$  standard deviation (SD). Data analysis was done by using T-test and two-way ANOVA assay (ANOVA). Data were analyzed by GraphPad Prism (version 7.03, GraphPad Software Inc, USA), and  $p < 0.0001$  was considered as statistically significant.

## Results and Discussion

In the current study, COL/PVA nanofibers were manufactured and optimized to eliminate the need for cross-linking step. The biocompatibility of scaffolds and their interactions with cells analyzed by seeding of HUC-MSCs on synthesized scaffolds.

### Characterization

#### FTIR Analysis

Chemical structure and interactions between different elements of synthesized scaffolds were investigated by Fourier-transform infrared spectroscopy (FTIR). Figure 2 illustrates the FTIR results for COL, PVA, un-cross-linked and GA cross-linked COL/PVA nanofibers. Any structural changes that might have occurred after being crosslink were identified and analyzed using FTIR spectroscopy. As seen, COL spectra (Figure 1, graphic of blue) showed two main peaks in 1700-1500  $\text{cm}^{-1}$  [35]. Amide I peak from C=O stretching vibrations and amide II peak from N-H

bending vibrations coupled with C-N stretching were appeared in the range of 1660-1630  $\text{cm}^{-1}$  and 1550-1570  $\text{cm}^{-1}$ , respectively. As expected, in the PVA spectrum (Figure 1, graphic of green), there was broad band from O-H group stretching vibration in the range of 3275-3250  $\text{cm}^{-1}$ . Furthermore, absorption bands related to asymmetric and symmetric stretching vibration of C-H group were appeared in the range of 2930-2940  $\text{cm}^{-1}$  and 2905-2910  $\text{cm}^{-1}$ , respectively. The band related to C=O group was appeared at 1650-1720  $\text{cm}^{-1}$ . The appeared band in 1656  $\text{cm}^{-1}$  is related to overlap of water bound with C=O bonding group. In addition, C-O stretching group was detected at wave number of 1035.5  $\text{cm}^{-1}$  and C=C group was detected at 1631.5  $\text{cm}^{-1}$  [36]. Figure 1 (black spectra) is spectrum of COL/PVA nanofibers. COL/PVA spectra showed the existence of O-H stretching and N-H stretching

groups at 3429- 3435  $\text{cm}^{-1}$ . In addition, creating physical cross linking between PVA hydroxyl groups with COL amide groups caused the intensity of O-H stretching peak and the weak amid I and II peaks. The C-H stretching group was detected in wave numbers of 2920.16-2930.16  $\text{cm}^{-1}$ . Cluster C=C stretching and C=O peaks were located at wave numbers 1650-1720  $\text{cm}^{-1}$  [30].

Figure 1 (red spectra) is spectrum of GA cross linked COL/PVA nanofibers. Absorption analysis results show that O-H bending and stretching group absorption peak at wave numbers 3429-3435  $\text{cm}^{-1}$  has been removed as a result of the inclusion of oxygen molecules in crosslinking. In addition, the intensity of the carbonyl peak in wave number range of 1650-1720  $\text{cm}^{-1}$  was also increased compared to the spectrum of uncross linked nanofibers [37,38].

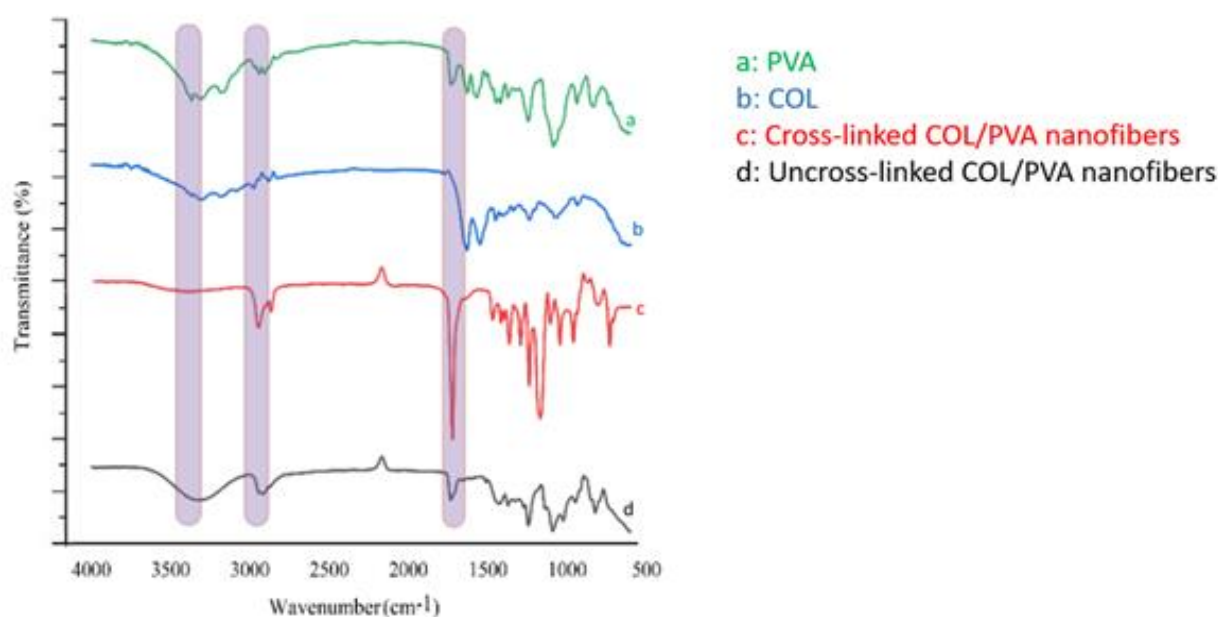


**Figure 1.** FTIR analysis of (a) PVA, (b) collagen, (c) GA cross linked COL/PVA nanofibers, (d) Un cross linked COL/PVA nanofibers

### SEM Images of COL/PVA Nanofibers

The SEM images of the COL/PVA nanofibers with different percentages of COL and PVA are depicted in Figure 2. Based on SEM images, all scaffolds had a three-dimensional porous structure. Diameter of the COL/PVA nanofibers with volume ratios of 20/80, 40/60, and 60/40

were around 100-500, 100-450, and 100-300  $\mu\text{m}$ , respectively. The quality of electrospinning process depends a large extent on the characteristics of prepared electrospinning solution. For example, higher COL concentrations disrupt the fallow of the electrospinning solution in the needle [39]. On the other hand, studies have proven that the presence of COL in tissue

engineering scaffolds has a significant effect on increasing the biocompatibility of synthesized scaffolds. Consistent with previously published studies, the average diameter of nanofibers decreases with increasing collagen percentage [39,40]. In this study, the average nanofiber

diameter was determined using ImageJ software by selecting 10 random points in the SEM images. The higher percentage of collagen in the electrospinning solution increases the viscosity of the solution and causes problems in its flow inside the needle [39,41].

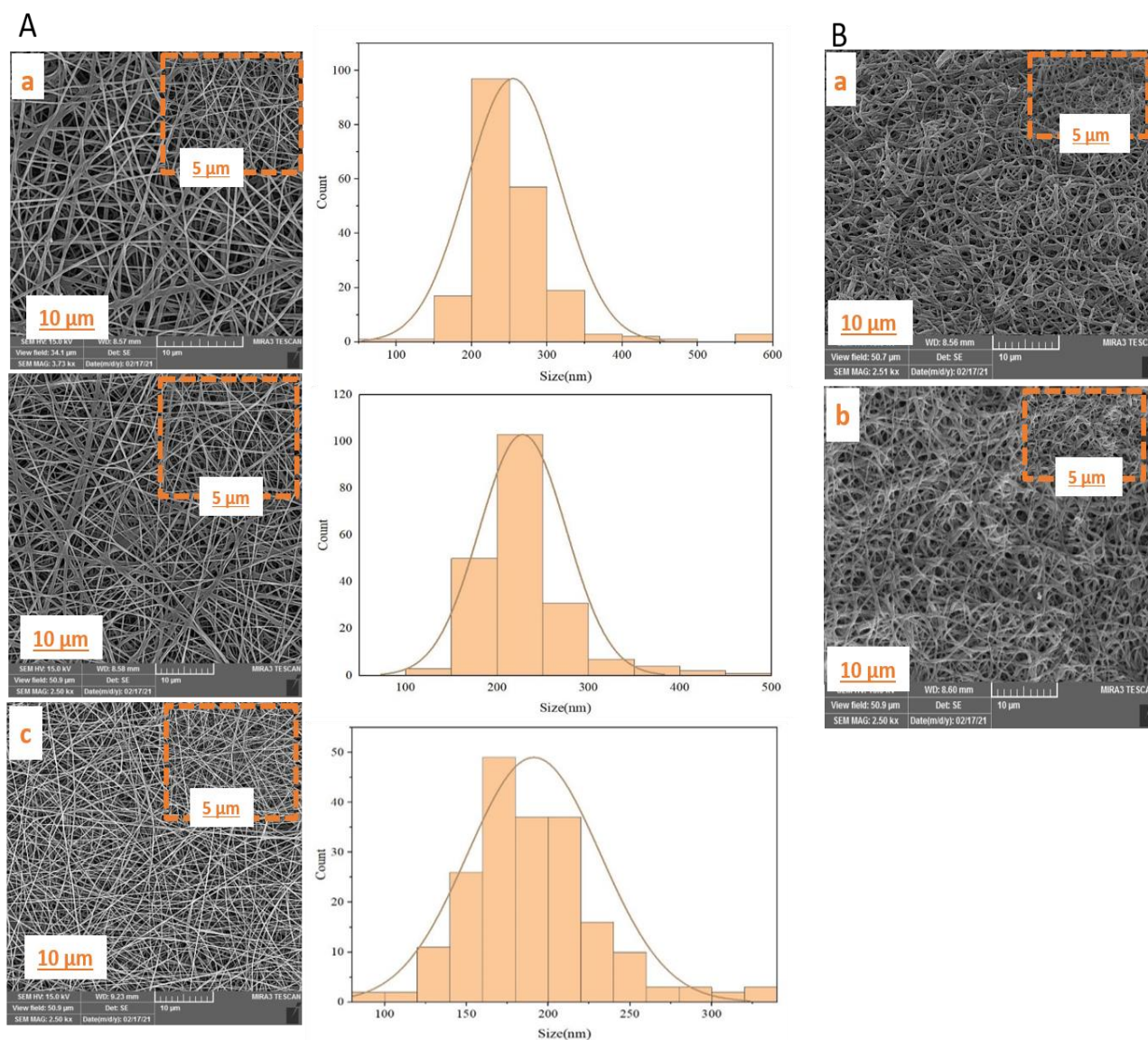


**Figure 2.** SEM images of (a) COL/PVA 20%, (b) COL/PVA 40%, (c) COL/PVA 60% un cross linked nanofibers. Average diameter and distribution of COL/PVA 20%, COL/PVA 40%, COL/PVA 60% un cross linked nanofibers determined by ImageJ. Results are presented as mean ± standard deviation

We found that the electrospinning ability of COL/PVA blends decreased drastically with increasing COL content of electrospinning solution. On the other hand, the COL presence in the structure of synthetic scaffolds has a very significant effect on improving the biocompatibility of scaffolds. Therefore, one of the important challenges in this research is to

achieve the optimal amount of COL in the scaffold structure.

### Mechanical Analysis

Endometrial scaffolds are artificial ECM structures to provide mechanical support for the uterus cells and vascular architecture for blood

perfusion. Generally, in all tissues the composition and organization of ECM determines the mechanical properties of the tissue. Soft tissues due their Young's modulus of approximately 1 MPa have high flexibility [42-44]. The mechanical properties of prepared nanofibers are strongly dependent on nanofibers structure and their interactions and also their surface morphology [45,46]. The tensile strain-stress curves of the 20%, 40%, 60%, and GA cross linked COL/PVA 20% electrospun nanofibers are shown in Figure 3 (a,b). As evident in the diagrams, by increasing the percentage of collagen in the nanofibers structure, the Young's

modulus of the produced structures increased. Actually, nanofibers contain a higher percentage of collagen have finer nanofibers that are more strongly connected to each other and thus have better mechanical properties. As expected, the mechanical features of nanofibers become much stronger due to GA cross linking process. This is while the strain of nanofibers due to the relative confusion of the created networks reduced by cross linking. It seems that the mechanical resistance of COL/PVA 60% without cross linker can also be sufficient for the endometrial tissue scaffolds.

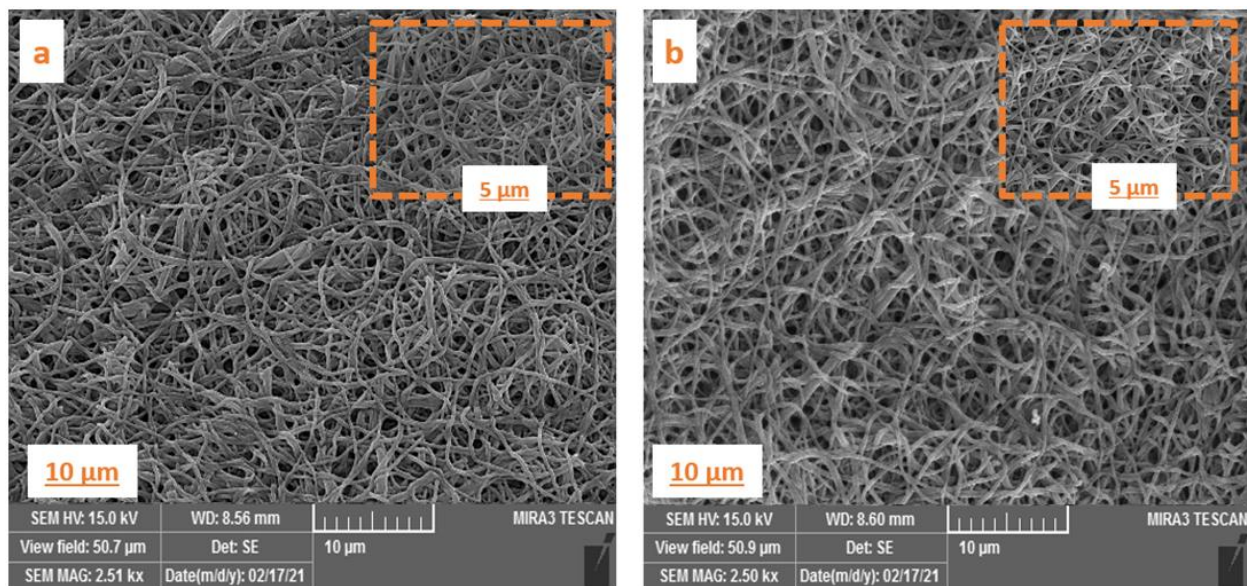


**Figure 3.** SEM images of (a) COL/PVA 20%, (b) COL/PVA 40% GA cross linked nanofibers

### Swelling and Degradation Evaluation

Biological fluids play a very important role in communicating between cells and transporting nutrients. Swelling rate of scaffolds show the synthesized scaffold ability in water absorption and retention. This property causes the absorption and retention of body fluids to facilitate cellular communication and mass transfer [47]. The swelling ratio in biomaterials is strongly dependent on the scaffold properties such as hydrophilicity, porosity, pore size pore shape, and cross-linking density of polymeric networks [48-50]. Therefore, designing scaffolds with optimal swelling behavior is essential for cell survival and ultimately better support for new tissue formation. The swelling ratio of the

prepared samples was investigated in PBS solution for 24, 48, and 72 hours. The experiments results are illustrated in Figure 4. As is clear in Figure 4 (a) the swelling ratio of prepared scaffolds within the 72 hours of the analysis, due to the hydrophilic nature of collagen and PVA is still high [51]. The swelling ratio in all synthesized nanofibers is increasing with time. Swelling ratio was significantly higher in GA cross linked 20% and 40% COL/PVA nanofibers compared to un cross linked 60% COL/PVA nanofibers. Moreover, a denser, and chaotic, dense, and stronger polymeric network with lower porosity was made by increasing the COL percentage in the COL/PVA nanofibers. Thus, its swelling ratio was decreased in un cross linked



60% COL/PVA nanofibers in comparison with cross linked 20% and 40% COL/PVA nanofibers. Biodegradability is another feature that can be investigated in the design and construction of tissue engineering scaffolds [52]. Scaffolds In vitro degradation rate was evaluated at 37 °C in PBS solution [53]. In Figure 4 (b), weight loss of prepared scaffold samples in certain time intervals is displayed. As it can be seen, the weight loss of un-cross-linked COL/PVA nanofibers (60%) is significantly higher compared to GA cross linked nanofibers. There was no significant difference in the biodegradation rate of GA cross linked (20%) and

(40%) COL/PVA nanofibers. After 21 days, the percentage of weight loss of un-cross-linked COL/PVA nanofibers (mean 66.33) was acceptable. Unlike uncross linked 60% COL/PVA nanofiber, un-cross-linked 20% and 40% COL/PVA nanofibers were degraded as soon as they came into contact with the water environment Figure 4. Probably, increasing the COL percentage in the structure of nanofibers will create denser networks in the structure of the scaffold, and this will optimize the biodegradability of nanofibers without the need for GA cross linker.

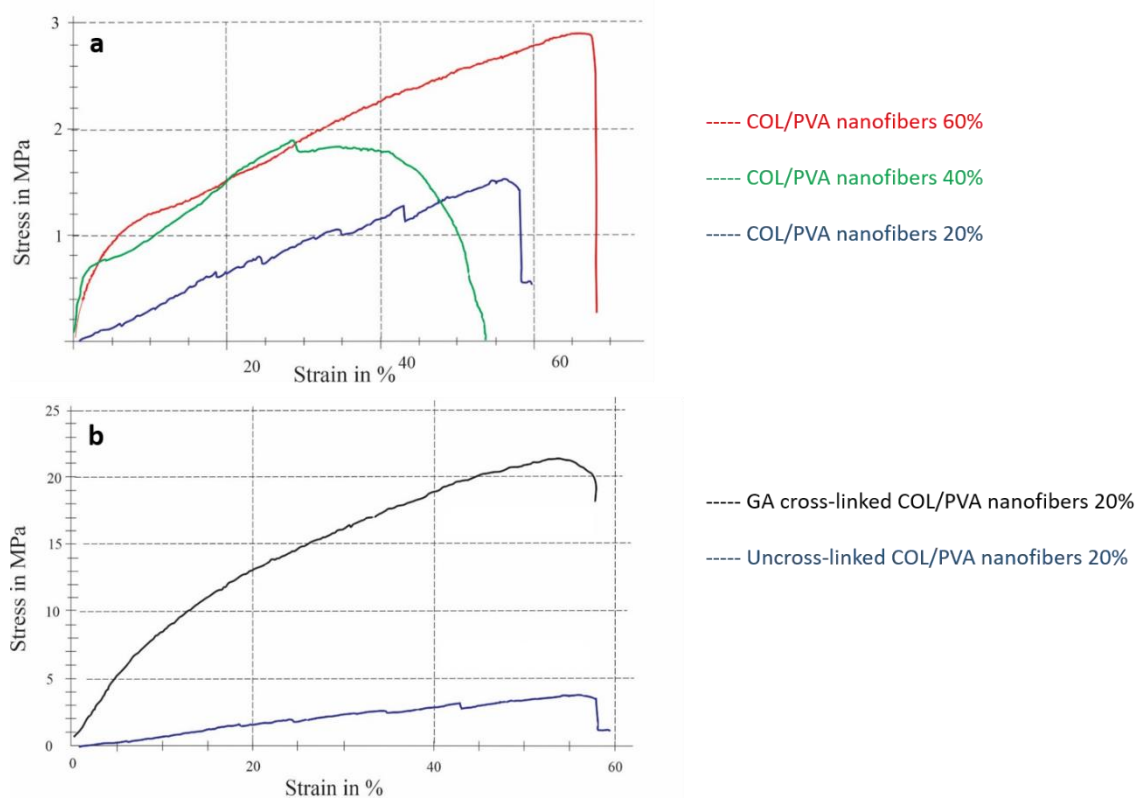


**Figure 4.** The stress-strain curves of (a) COL/PVA 20%, COL/PVA 40%, COL/PVA 60% un cross linked nanofibers and (b) COL/PVA 20% un cross linked and GA cross linked nanofibers. Data are expressed as mean  $\pm$  standard deviation (n = 3)

### Biological Evaluation of the Scaffolds

To assess the biocompatibility of the synthesized scaffolds, MTT assay was used according to ISO 10993-5:1999 standard [54]. In this analysis, the effects of GA cross linked 20%, 40% nanofibers and un-cross-linked 60% COL/PVA nanofibers on

viability and proliferation of HUC-MSCs were examined (Figure 5). In this method the optical density (OD value) was measured as the mitochondrial redox activity of living cells. In this study cell viability of control and sample groups was measured after 24, 48, and 72 hours of incubation. As seen in Figure 5, the cell viability

in all prepared scaffold samples improved by over time. As previous studies have shown, the COL/PVA nanofiber scaffolds showed high biocompatibility [19,55-56]. HUC-MSCs on cell culture plates without scaffolds were considered as the control group. The 60% un cross linked COL/PVA nanofibers compared with 20% and 40% GA cross-linked nanofibers, had more cell viability. As expected, by increasing the COL percentage in the synthesized scaffolds and removal GA, synthesized scaffolds biocompatibility increased [57]. In addition, HUC-MSC cells seeded on the un-cross-linked 60% COL/PVA nanofibers had highest proliferation rate. Studies have shown that higher levels of

apoptosis, poor cell attachment to scaffold and spread of residual cells could be the reason for the reduced biocompatibility of GA cross-linked COL/PVA nanofiber scaffolds [24]. After culturing for three days, the proliferation activity of control group was decreased through contact inhibition. While, cells seeded in COL/PVA nanofiber scaffolds due to high surface area-to-volume ratio of scaffolds maintained high proliferation activity. According to the results obtained from the previous sections, high biocompatibility and acceptable physicochemical properties of 60% un-cross-linked COL/PVA nanofibers (60%) the study was continued with these nanofibers.

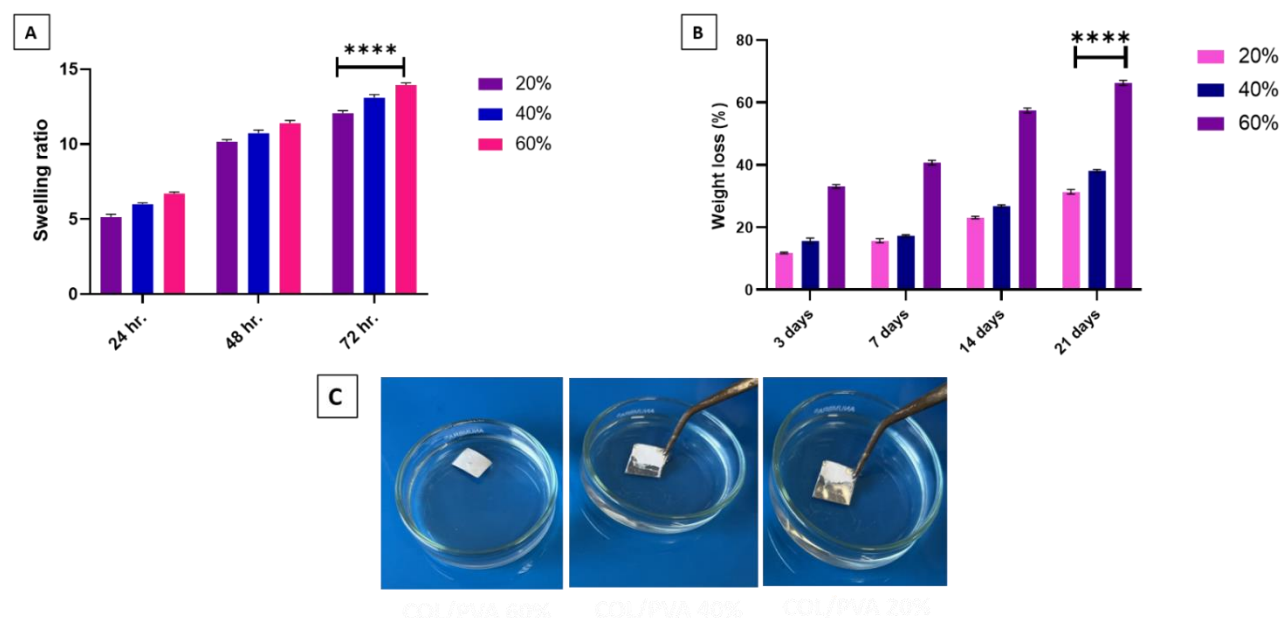


**Figure 5. A.** Swelling behavior of the GA cross linked COL/PVA 20%, COL/PVA 40% GA and un cross linked COL/PVA 60% nanofibers in PBS (at pH=7.4) during 15 days). Data are expressed as mean  $\pm$  standard deviation (n = 3) (\*\*\*\*p < 0.0001). **B.** The degradation graph of COL/PVA 20%, COL/PVA 40% GA cross linked and un cross linked COL/PVA 60% nanofibers in 30 days. The medium was replaced with a fresh medium every 4 days. The degradation process was fulfilled at 37°C. Data are expressed as mean  $\pm$  standard deviation (n = 3). **C.** un cross linked COL/PVA 60% nanofibers and un cross linked COL/PVA 20% and 40% nanofibers

### Morphological Characterization of UCMSCs on COL/PVA Nanofiber Scaffolds and Cell Adhesion Study

The morphology of cells on the prepared scaffolds and the quality of cell adhesion to the scaffold is checked by SEM imaging. The results showed that HUC-MSCs had well cell to the nanofiber scaffolds attachment and normal round-shape morphology (Figure 6 , 7). Good cell

adhesion occurred as a result of the ability of synthesized scaffolds to successfully mimic the function of natural ECM. COL contains the arginine-glycine-aspartic acid (RGD) sequences that are useful for promoting cell attachment and proliferation [58,59]. This is why the presence of collagen in the scaffold structure has a significant impact on its biocompatibility. In fact, cell adhesion to the scaffold surface is strongly influenced by various properties such as surface

roughness, biodegradability, porous structure, and swelling properties of the scaffold. Cells apparently prefer to adhere and spread on

uniform morphology of surface in dense scaffolds.

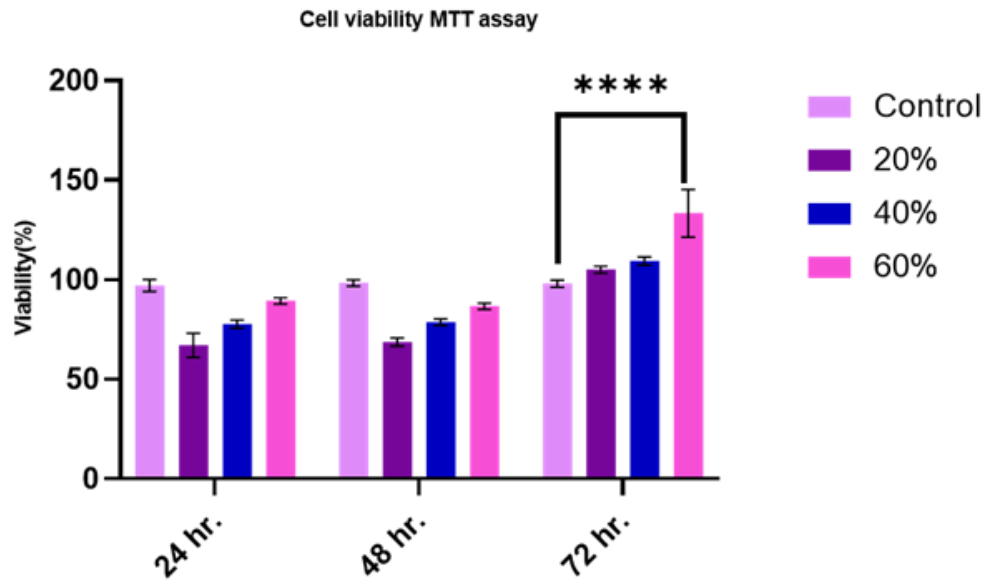


**Figure 6.** MTT assay for HUC-MSCs cultured on the routine medium (control), GA cross linked COL/PVA 20%, COL/PVA 40% and un cross linked COL/PVA 60% nanofibers for 24, 48, and 72 hr. (\*\*\*\* $p < 0.0001$ )

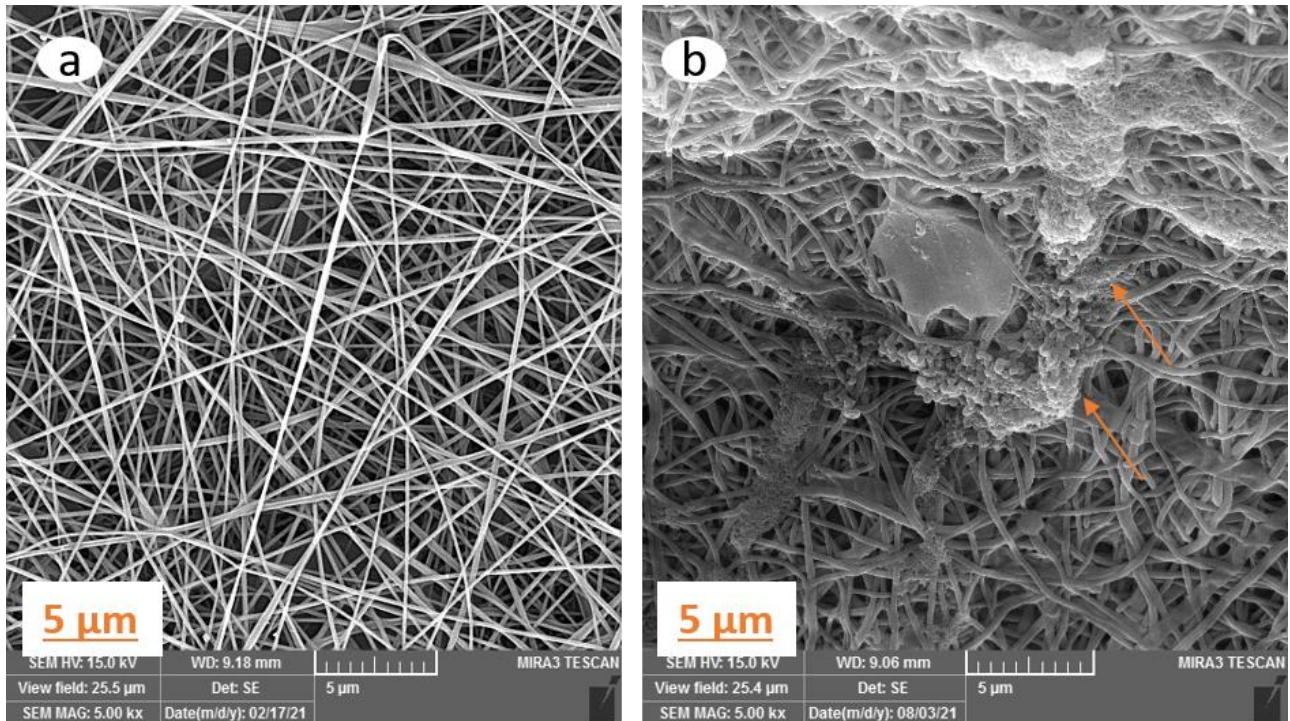


**Figure 7.** Scanning electron microscopy images of HUC-MSCs following 3 days of culture throughout the un cross linked COL/PVA 60% nanofibers. (a) COL/PVA 60% scaffold before cell seeding, (b) COL/PVA 60% scaffold after cell seeding

## Conclusion

In this study, COL/PVA nanofiber scaffolds were successfully fabricated. By optimizing the ratio of COL to PVA it was possible to achieve desirable biological and physicochemical properties in synthesized scaffolds. Increasing the COL percentage and removing glutaraldehyde had a significant effect on increasing the biocompatibility of COL/PVA nanofiber scaffolds.

## Acknowledgments

This work was supported by the Tabriz University of Medical Science–Department of Medicinal Chemistry, Pharmacy School- (Grant No. 64761).

## Authors' Contributions

All authors contributed to data analysis, drafting, and revising of the paper and agreed to be responsible for all the aspects of this work.

## Conflict of Interest

We have no conflicts of interest to disclose.

## ORCID

Soodabeh Davaran

<https://orcid.org/0000-0002-7072-2362>

## References

- [1]. Cervelló I., Santamaría X., Miyazaki K., Maruyama T., Simón C., in *Seminars in Reproductive Medicine*. 366 (Thieme Medical Publishers) [Google Scholar], [Publisher]
- [2]. Sittadjody S., Criswell T., Jackson J.D., Atala A., Yoo J., Regenerative medicine approaches in bioengineering female reproductive tissues, *Reproductive Sciences*, 2021, **28**:1573 [Crossref], [Google Scholar], [Publisher]
- [3]. Dadashzadeh A., Moghassemi S., Shavandi A., Amorim C.A., A review on biomaterials for ovarian tissue engineering, *Acta Biomaterialia*, 2021, **135**:48 [Crossref], [Google Scholar], [Publisher]
- [4]. Vig K., Chaudhari, A., Tripathi S., Dixit S., Sahu R., Pillai S., Dennis V.A., Singh S.R., Advances in skin regeneration using tissue engineering, *International Journal of Molecular Sciences*, 2017, **18**:789 [Crossref], [Google Scholar], [Publisher]
- [5]. Salvatori M., Peloso A., Katari R., Orlando G., Regeneration and bioengineering of the kidney: current status and future challenges, *Current Urology Reports*, 2014, **15**:1 [Crossref], [Google Scholar], [Publisher]
- [6]. Gu X., Ding F., Williams D.F., Neural tissue engineering options for peripheral nerve regeneration, *Biomaterials*, 2014, **35**:6143 [Crossref], [Google Scholar], [Publisher]
- [7]. Jahanbani Y., Shafiee S., Davaran S., Roshangar L., Ahmadian E., Eftekhari A., Dolati S., Yousefi M., Stem cells technology as a platform for generating reproductive system organoids and treatment of infertility-related diseases, *Cell Biology International*, 2022, **46**:512 [Crossref], [Google Scholar], [Publisher]
- [8]. Jahanbani Y., Davara, S., Ghahremani-Nasab M., Aghebati-Maleki L., Yousefi M., Scaffold-based tissue engineering approaches in treating infertility, *Life Sciences*, 2020, **240**:117066 [Crossref], [Google Scholar], [Publisher]
- [9]. Sullivan R., Dailey T., Duncan K., Abel N., Borlongan C.V., Peripheral nerve injury: stem cell therapy and peripheral nerve transfer, *International Journal of Molecular Sciences*, 2016, **17**:2101 [Crossref], [Google Scholar], [Publisher]
- [10]. Marcheque J., Bussolati B., Csete M., Perin L., Concise reviews: stem cells and kidney regeneration: an update, *Stem Cells Translational Medicine*, 2019, **8**:82 [Crossref], [Google Scholar], [Publisher]
- [11.] Hu X.M., Zhang Q., Zhou R.X., Wu Y.L., Li Z.X., Zhang D.Y., Yang Y.C., Yang R.H., Hu Y.J., Xiong K., Programmed cell death in stem cell-based therapy: Mechanisms and clinical applications, *World Journal of Stem Cells*, 2021, **13**:386 [Crossref], [Google Scholar], [Publisher]
- [12]. Xue Y., Bai R., Dong Y., Recent advances of biomaterials in stem cell therapies, *Nanotechnology*, 2022, **33**:132501 [Crossref], [Google Scholar], [Publisher]
- [13]. Fan Z., Li X., Niu H., Guan J., Myocardial Regenerative Medicine, *Polymeric Biomaterials*

- for Tissue Regeneration: From Surface/Interface Design to 3D Constructs, 2016, 353 [Crossref], [Google Scholar], [Publisher]
- [14]. Chen Y., Pal S., Hu Q., Recent advances in biomaterial-assisted cell therapy, *Journal of Materials Chemistry B*, 2022, **10**:7222 [Crossref], [Google Scholar], [Publisher]
- [15]. Paternoster J.L., Vranckx J.J., State of the art of clinical applications of tissue engineering in 2021, *Tissue Engineering Part B: Reviews*, 2022, **28**:592 [Crossref], [Google Scholar], [Publisher]
- [16]. Jahanbani Y., Memarmaher B., Ghaleh H., Agbolaghi S., Jalili K., Abbaspoor S., Abbasi F., Three-dimensional macro/mesoporosity developments in polydimethylsiloxane, *International Journal of Polymeric Materials and Polymeric Biomaterials*, 2018, **67**:847 [Crossref], [Google Scholar], [Publisher]
- [17]. Chen M., Jiang R., Deng N., Zhao X., Li X., Guo C., Natural polymer-based scaffolds for soft tissue repair, *Frontiers in Bioengineering and Biotechnology*, 2022, **10**:954699 [Crossref], [Google Scholar], [Publisher]
- [18]. Kohane D.S., Langer R., Polymeric biomaterials in tissue engineering, *Pediatric Research*, 2008, **63**:487 [Crossref], [Google Scholar], [Publisher]
- [19]. Abedi G., Sotoudeh A., Soleymani M., Shafiee A., Mortazavi P., Aflatoonian M.R., A collagen–poly (vinyl alcohol) nanofiber scaffold for cartilage repair, *Journal of Biomaterials Science, Polymer Edition*, 2011, **22**:2445 [Crossref], [Google Scholar], [Publisher]
- [20]. Zuber M., Zia F., Zia K.M., Tabasum S., Salman M., Sultan N., Collagen based polyurethanes—A review of recent advances and perspective, *International Journal of Biological Macromolecules*, 2015, **80**:366 [Crossref], [Google Scholar], [Publisher]
- [21]. Ehrmann A., Non-toxic crosslinking of electrospun gelatin nanofibers for tissue engineering and biomedicine—a review, *Polymers*, 2021, **13**:1973 [Crossref], [Google Scholar], [Publisher]
- [22]. Baker M.I., Walsh S.P., Schwartz Z., Boyan B.D., A review of polyvinyl alcohol and its uses in cartilage and orthopedic applications, *Journal of Biomedical Materials Research Part B: Applied Biomaterials*, 2012, **100**:1451 [Crossref], [Google Scholar], [Publisher]
- [23]. Liu Y., Ma L., Gao C., Facile fabrication of the glutaraldehyde cross-linked collagen/chitosan porous scaffold for skin tissue engineering, *Materials Science and Engineering: C*, 2012, **32**:2361 [Crossref], [Google Scholar], [Publisher]
- [24]. Gough J.E., Scotchford C.A., Downes S., Cytotoxicity of glutaraldehyde crosslinked collagen/poly (vinyl alcohol) films is by the mechanism of apoptosis, *Journal of Biomedical Materials Research*, 2002, **61**:121 [Crossref], [Google Scholar], [Publisher]
- [25]. Sung H.W., Huang R.N., Huang L.L., Tsai C.C., In vitro evaluation of cytotoxicity of a naturally occurring cross-linking reagent for biological tissue fixation, *Journal of Biomaterials Science, Polymer Edition*, 1999, **10**:63 [Crossref], [Google Scholar], [Publisher]
- [26]. Saha S., Roy P., Corbitt C., Kakar S.S., Application of stem cell therapy for infertility, *Cells*, 2021, **10**:1613 [Crossref], [Google Scholar], [Publisher]
- [27]. Volarevic V., Bojic S., Nurkovic J., Volarevic A., Ljubic B., Arsenijevic N., Lako M., Stojkovic M., Stem cells as new agents for the treatment of infertility: current and future perspectives and challenges, *BioMed Research International*, 2014, **2014** [Crossref], [Google Scholar], [Publisher]
- [28]. Sudirman S., Karo A.K., Sukaryo S.G., Adistiana K.D., Dahlan K., Synthesis of nanofiber from polyvinyl alcohol (PVA)-Collagen using electrospinning methods, *Indonesian Journal of Applied Chemistry*, 2020, **21**:55 [Crossref], [Google Scholar], [Publisher]
- [29]. Anaya Mancipe J.M., Lopes Dias M., Moreira Thiré R.M.D.S., Type I collagen–poly (vinyl alcohol) electrospun nanofibers: FTIR study of the collagen helical structure preservation, *Polymer-Plastics Technology and Materials*, 2022, **61**:846 [Crossref], [Google Scholar], [Publisher]
- [30]. Zhang X., Tang K., Zheng, X., Electrospinning and crosslinking of COL/PVA nanofiber-microsphere containing salicylic acid for drug delivery, *Journal of Bionic Engineering*, 2016, **13**:143 [Crossref], [Google Scholar], [Publisher]
- [31]. Vega S.L., Kwon M.Y., Burdick J.A., Recent advances in hydrogels for cartilage tissue

- engineering, *European Cells & Materials*, 2017, **33**:59 [Crossref], [Google Scholar], [Publisher]
- [32]. Sala R.L., Kwon M.Y., Kim M., Gullbrand S.E., Henning E.A., Mauck R.L., Camargo E.R., Burdick J.A., Thermosensitive poly (N-vinylcaprolactam) injectable hydrogels for cartilage tissue engineering, *Tissue Engineering Part A*, 2017, **23**:935 [Crossref], [Google Scholar], [Publisher]
- [33]. Dai Z., Ronholm J., Tian Y., Sethi B., Cao X., Sterilization techniques for biodegradable scaffolds in tissue engineering applications, *Journal of Tissue Engineering*, 2016, **7**:2041731416648810 [Crossref], [Google Scholar], [Publisher]
- [34]. Ghandforoushan P., Hanaee J., Aghazadeh Z., Samiei M., Navali A.M., Khatibi A., Davaran S., Novel nanocomposite scaffold based on gelatin/PLGA-PEG-PLGA hydrogels embedded with TGF- $\beta$ 1 for chondrogenic differentiation of human dental pulp stem cells in vitro, *International Journal of Biological Macromolecules*, 2022, **201**:270 [Crossref], [Google Scholar], [Publisher]
- [35]. Bolgen N., Çetinkaya Z., Demir D., Fish skin isolated collagen cryogels for tissue engineering applications: Purification, synthesis and Characterization, *Journal of the Turkish Chemical Society Section A: Chemistry*, 2016, **3**:329 [Crossref], [Google Scholar], [Publisher]
- [36]. Zhang Z., Liu Y., Lin S., Wang Q., Preparation and properties of glutaraldehyde crosslinked poly (vinyl alcohol) membrane with gradient structure, *Journal of Polymer Research*, 2020, **27**:1 [Crossref], [Google Scholar], [Publisher]
- [37]. Mansur H.S., Sadahira C.M., Souza A.N., Mansur A.A.J.M.S., C E., FTIR spectroscopy characterization of poly (vinyl alcohol) hydrogel with different hydrolysis degree and chemically crosslinked with glutaraldehyde, 2008, **28**:539 [Crossref], [Google Scholar], [Publisher]
- [38]. Duraipandy N., Lakra R., Srivatsan K.V., Ramamoorthy U., Korrapati P.S., Kiran M.S.J.o.M.C.B., Plumbagin caged silver nanoparticle stabilized collagen scaffold for wound dressing, 2015, **3**:1415 [Crossref], [Google Scholar], [Publisher]
- [39]. Sudirman S., Karo A.K., Sukaryo S.G., Adistiana K.D., Dahlan K., Synthesis of nanofiber from polyvinyl alcohol (PVA)-Collagen using electrospinning methods, *Jurnal Kimia Terapan Indonesia*, 2020, **21**:55 [Crossref], [Google Scholar], [Publisher]
- [40]. Sai K.P., Babu M., Studies on Rana tigerina skin collagen, *Comparative Biochemistry and Physiology Part B: Biochemistry and Molecular Biology*, 2001, **128**:81 [Crossref], [Google Scholar], [Publisher]
- [41]. Rupiasih N.N., Pranastia D.A.S., Sumadiyasa M., Vidyasagar P., Effect of collagen concentration on morphology of PVA/chitosan fibers made by electrospinning method, *Jurnal Neutrino: Jurnal Fisika dan Aplikasinya*, 2023, **15**:62 [Crossref], [Google Scholar], [Publisher]
- [42]. Raia N.R., McGill M., Marcet T., Yucha S.E.V., Kaplan D.L., *Biomaterials Science*, 2020, 1399 (Elsevier, 2020). [Crossref], [Google Scholar], [Publisher]
- [43]. Skeldon G., Lucendo-Villarín B., Shu W., Three-dimensional bioprinting of stem-cell derived tissues for human regenerative medicine, *Philosophical Transactions of the Royal Society B: Biological Sciences*, 2018, **373**:20170224 [Crossref], [Google Scholar], [Publisher]
- [44]. Akhtar R., Sherratt M.J., Cruickshank J.K., Derby B., Characterizing the elastic properties of tissues, *Materials Today*, 2011, **14**:96 [Crossref], [Google Scholar], [Publisher]
- [45]. Fathurochman F., Wuriantika M.I., Santjojo D.J.D.H., Nurhuda M., Mechanical, degradation rate, and antibacterial properties of a collagen-chitosan/PVA composite nanofiber, *Materials Research Express*, 2023, **10**:025401 [Crossref], [Google Scholar], [Publisher]
- [46]. Lee K.H., Kim H.Y., Ryu Y.J., Kim K.W., Choi S.W., Mechanical behavior of electrospun fiber mats of poly (vinyl chloride)/polyurethane polyblends, *Journal of Polymer Science Part B: Polymer Physics*, 2003, **41**:1256 [Crossref], [Google Scholar], [Publisher]
- [47]. Safari B., Aghanejad A., Kadkhoda J., Aghazade M., Roshangar L., Davaran S., Biofunctional phosphorylated magnetic scaffold for bone tissue engineering, *Colloids and Surfaces B: Biointerfaces*, 2022, **211**:112284 [Crossref], [Google Scholar], [Publisher]

- [48]. Felfel R.M., Gideon-Adeniyi M.J., Hossain K.M.Z., Roberts G.A., Grant D.M., Structural, mechanical and swelling characteristics of 3D scaffolds from chitosan-agarose blends, *Carbohydrate Polymers*, 2019, **204**:59 [Crossref], [Google Scholar], [Publisher]
- [49]. Çay A., Miraftab M., Kumbasar E.P.A., Characterization and swelling performance of physically stabilized electrospun poly (vinyl alcohol)/chitosan nanofibres, *European Polymer Journal*, 2014, **61**:253 [Crossref], [Google Scholar], [Publisher]
- [50]. Cojocar F.D., Balan V., Popa M.I., Lobiuc A., Antoniac A., Antoniac I.V., Verestiuc L., Biopolymers–calcium phosphates composites with inclusions of magnetic nanoparticles for bone tissue engineering, *International Journal of Biological Macromolecules*, 2019, **125**:612 [Crossref], [Google Scholar], [Publisher]
- [51]. Zhou T., Chen S., Ding X., Hu Z., Cen L., Zhang X., Fabrication and characterization of collagen/PVA dual-layer membranes for periodontal bone regeneration, *Frontiers in Bioengineering and Biotechnology*, 2021, **9**:630977 [Crossref], [Google Scholar], [Publisher]
- [52]. Bitar K.N., Zakhem E., Design strategies of biodegradable scaffolds for tissue regeneration, *Biomedical Engineering and Computational Biology*, 2014, **6**:BECB. S10961 [Crossref], [Google Scholar], [Publisher]
- [53]. Echeverria Molina M.I., Malollari, K.G., Komvopoulos, K., Design challenges in polymeric scaffolds for tissue engineering, *Frontiers in Bioengineering and Biotechnology*, 2021, **9**:617141 [Crossref], [Google Scholar], [Publisher]
- [54]. Kamal A.F., Iskandriati D., Dilogo I.H., Siregar N.C., Hutagalung E.U., Susworo R., Yusuf A.A., Bachtiar A., Biocompatibility of various hydroxyapatite scaffolds evaluated by proliferation of rat's bone marrow mesenchymal stem cells: an in vitro study, *Medical Journal of Indonesia*, 2013, **22**:202 [Crossref], [Google Scholar], [Publisher]
- [55]. Lin H.Y., Tsai W.C., Chang S.H., Collagen-PVA aligned nanofiber on collagen sponge as bi-layered scaffold for surface cartilage repair, *Journal of Biomaterials Science, Polymer Edition*, 2017, **28**:664 [Crossref], [Google Scholar], [Publisher]
- [56]. Karthick S.A., Ragavi T., Naresh K., Sreekanth P.R., A study on collagen-PVA and chitosan-PVA nanofibrous matrix for wound dressing application, *Materials Today: Proceedings*, 2022, **56**:1347 [Crossref], [Google Scholar], [Publisher]
- [57]. Senthil R., Berly R., Bhargavi Ram T., Gobi N., Electrospun poly (vinyl) alcohol/collagen nanofibrous scaffold hybridized by graphene oxide for accelerated wound healing, *The International Journal of Artificial Organs*, 2018, **41**:467 [Crossref], [Google Scholar], [Publisher]
- [58]. Parenteau-Bareil R., Gauvin R., Berthod F., Collagen-based biomaterials for tissue engineering applications, *Materials*, 2010, **3**:1863 [Crossref], [Google Scholar], [Publisher]
- [59]. Radhakrishnan S., Nagarajan S., Bechelany M., Kalkura S.N., Collagen based biomaterials for tissue engineering applications: A review, *Processes and Phenomena on the Boundary between Biogenic and Abiogenic Nature*, 2020, **3** [Crossref], [Google Scholar], [Publisher]



#### HOW TO CITE THIS ARTICLE

Y. Jahanbani, S. Davaran, Mehdi Yousefi, L. Roshangar, P. bastani, J. kadhoda. Fabrication and Characterization of COL/PVA Nanofiber Scaffolds for Soft Tissue Engineering. *Chem. Methodol.*, 2024, 8(5) 386-400

DOI: <https://doi.org/10.48309/chemm.2024.455838.1794>

URL: [https://www.chemmethod.com/article\\_197038.html](https://www.chemmethod.com/article_197038.html)